# CELSR3 deficiency leads to tic-related behaviors and dopaminergic alterations in the striatum

Roberto Cadeddu[1], Giulia Braccagni[1], Teresa Musci[1],
Ignazio S Piras[2], Collin J Anderson[3-5], Mario R Capecchi[6],
Matthew J Huentelman[2], Philip J Moos[1], Marco Bortolato[1]

1. Department of Pharmacology and Toxicology, College of Pharmacy, University of Utah, Salt Lake City, UT, USA
2. Neurogenomics Division, Translational Genomics Research Institute (TGen), Phoenix (AZ), USA
3. Department of Neurology, School of Medicine, University of Utah, Salt Lake City, Utah, USA
4. School of Medical Sciences, University of Sydney, Camperdown, Australia
5. School of Biomedical Engineering, University of Sydney, Camperdown, Australia
6. Department of Human Genetics, College of Medicine, University of Utah, Salt Lake City, UT, USA

**Running title**: *Celsr3* deficiency leads to Tourette-like abnormalities

**Corresponding author:**

**Marco Bortolato, MD PhD**

Dept. of Pharmacology & Toxicology
College of Pharmacy
University of Utah
L.S. Skaggs Hall, Room 3916
30 S 2000 E
Salt Lake City, UT 84112
USA
e-mail: marco.bortolato@utah.edu

**Abstract**

The gene *CELSR3* (cadherin EGF LAG seven-pass-G-type receptor 3) has been recently recognized as a high-confidence risk factor for Tourette syndrome (TS) Here, we characterized the behavioral phenotypes of *Celsr3* mutant mice to verify whether the deficiency of this gene is associated with TS predisposition. *Celsr3* mutant mice displayed tic-like grooming stereotypies and jerks, as well as sensorimotor gating deficits, which were opposed by TS therapies. Single-nucleus transcriptomic analyses revealed that *Celsr3* mutants featured a unique group of eccentric striatal projection neurons. Notably, the *Drd3* gene, encoding the dopamine $D_3$ receptor, was significantly upregulated in these cells as well as striosomal $D_1$-positive neurons, while it was reduced in calretinin-positive GABAergic interneurons. Activating and blocking $D_3$ receptors amplified or decreased tic-like jerks and stereotypies *in Celsr3*-deficient mice, respectively. These findings suggest that modifications of $D_3$ receptor distribution across various striatal cell populations contribute to the tic-like responses associated with *Celsr3* deficiency.

**Keywords**: *CELSR3*, tics, animal models, mouse, transcriptomics, single-nuclei transcriptomics

## INTRODUCTION

Tics are partially involuntary, highly repetitive movements or vocalizations with variable intensity and complexity. They are often a significant source of disability, negatively affecting social and emotional adjustment, educational attainment, and overall quality of life [1–5]. The most debilitating tic disorder is Tourette syndrome (TS), a neurodevelopmental disorder characterized by multiple motor tics and at least one vocal tic for over a year [6]. TS is estimated to affect approximately 0.5% of children [7] and is notably more prevalent in boys, with a male-to-female ratio of ~3:1 [8]. The typical course of TS features a clinical onset around six years, followed by a progressive exacerbation of tic severity and a gradual amelioration after puberty [9,10]. The trajectory of TS is also influenced by comorbid psychiatric conditions such as obsessive-compulsive disorder (OCD), attention-deficit hyperactivity disorder (ADHD), anxiety, and depression [11–14]. The primary pharmacological treatment for TS treatment involves the use of the $D_2$ receptor antagonist haloperidol or the $\alpha_2$ adrenergic receptor agonist clonidine [15]; however, the efficacy of these treatments is inconsistent, and their utility is hampered by significant adverse effects [16,17], underscoring the critical need to identify novel therapeutic targets.

The pathophysiology of tics is rooted in alterations in the cortico-striatal-thalamo-cortical circuitry [18]. In particular, tics are generally posited to arise from aberrant disinhibition foci in the dorsal striatum [19]. Nevertheless, the molecular mechanisms underlying these alterations remain elusive. Given the strong genetic predisposition of TS and other tic disorders, many attempts to identify their molecular underpinnings have leaned on genetic studies. However, most genetic contributors to tic development are still undiscovered. Recently, several studies on *de novo* mutations highlighted the gene *CELSR3* [cadherin epidermal growth factor laminin G seven-pass G-type receptor 3] as one of the first high-confidence TS risk genes [20-22]. This gene encodes a membrane receptor in the cadherin superfamily, which contains seven transmembrane domains and a large ectodomain interacting with neighboring cells [23]. *CELSR3* is broadly expressed in the CNS, where it regulates the formation of neural pathways and basal ganglia [24,25].

Despite this correlational evidence, it remains unclear whether loss-of-function *CELSR3* mutations lead to tics and other deficits. To elucidate this issue, here we analyzed whether *Celsr3*-deficient mice [26] may exhibit tic-like responses and striatal abnormalities. Given that homozygous knock-out mice for this gene were shown to die rapidly after birth [27], phenotypes were assessed in *Celsr3* heterozygous (HZ) and wild-type (WT) control mice. This HZ genotype aligns with the finding that *CELSR3 de novo* mutations (typically affecting only one allele) have been observed in TS-affected subjects [20–22].

We first employed a targeted behavioral phenotyping approach in *Celsr3* HZ pups and juvenile mice (as described in Figure 1) to monitor subtle changes in spontaneous and stress-exacerbated motor behaviors. Then, we assayed various behavioral responses related to comorbid disorders. The predictive validity of this animal model was examined comprehensively by testing their responsiveness to multiple TS therapies based on distinct mechanisms of action. Lastly, we conducted transcriptomic analyses of the striata from *Celsr3*-deficient mice to gain insight into potential mechanisms underlying the emergence of TS-related phenotypes resulting from the deficiency of this protocadherin.

## RESULTS

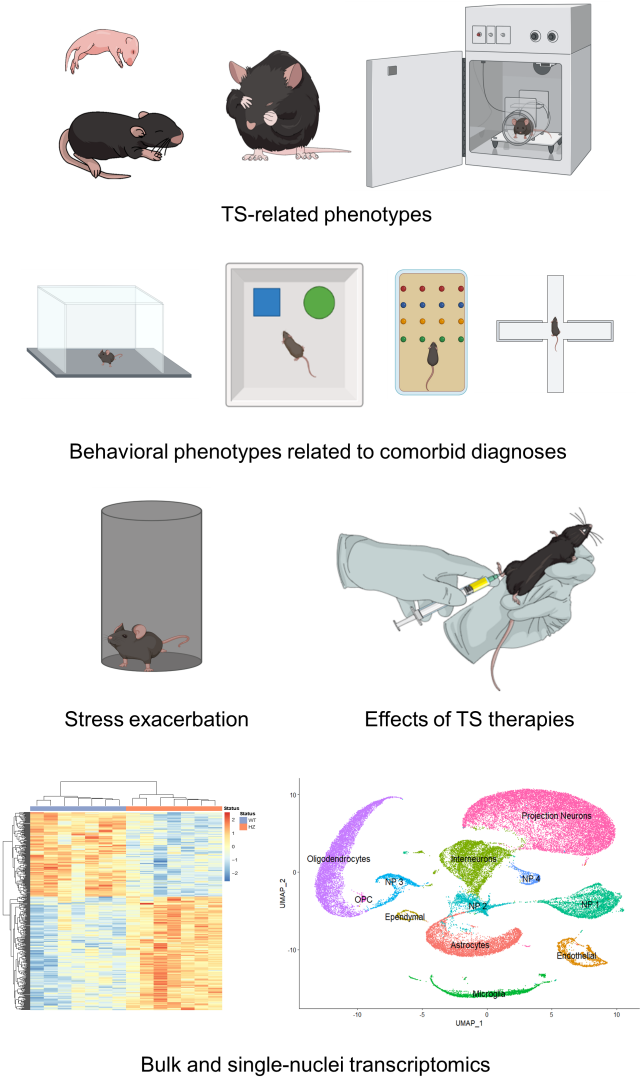


**Figure 1. Schematic representation of the procedures used in the present study.** The face validity of *Celsr3* heterozygous (HZ) mice with respect to tic disorders and related behavioral deficits was assessed at different developmental stages (neonates, adolescents, and adults, using different cohorts of mice to avoid carryover stress), in comparison with wild-type (WT) littermates. Separate groups of juvenile mice were tested to measure behavioral responses related to common comorbid diagnoses, such as anxiety and obsessive-compulsive disorder. The effects of acute stress and pharmacological treatments were also tested in juvenile mice to determine the predictive validity of *Celsr3* HZ mice. Following these analyses, we conducted bulk and single-nucleus transcriptomic profiling of the striatum of *Celsr3* HZ and WT mice to identify neurobiological aberrances associated with Celsr3 deficiency.

The following descriptions provide a brief summary of the results. For a comprehensive account and all statistical details, please refer to Supplemental results.

***Celsr3* HZ Mice Display TS-Related Behavioral Alterations**. We first examined the temporal trajectory of the behavioral responses of *Celsr3* HZ mice compared to their WT littermates, testing separate groups of mice at different developmental stages (see Supplemental Results for detailed information). Throughout the first postnatal week, WT and HZ male and female newborns exhibited no overt difference in motor responses and maternal separation-induced ultrasonic vocalizations (Figures S1A-S1C). To test whether *Celsr3*-deficient mice exhibited TS-related behavioral responses, we assessed tic-like jerks and stereotypies, as well as their prepulse inhibition (PPI) of the acoustic startle, which is typically defective in TS patients [28]. This evaluation was conducted in male and female HZ and WT littermates, using two separate cohorts of mice aged 21 (after weaning) and 42 days (juvenile stage), respectively, to avoid potential stress carryover effects (Figure 2). These experiments revealed that male and female 21-day-old *Celsr3*-deficient mice exhibited more spontaneous self-grooming responses than their WT counterparts (Figure 2A); however, no significant changes in the frequency of body and head jerks, chewing stereotypies, or eye blinking were observed at this stage (Figures 2B-2D). Unlike males, female weanling HZ mice showed a decline in digging activities compared to WT littermates (Figure 2E). While acoustic startle amplitude was equivalent across all experimental groups (Figure 2F), PPI deficits across all loudness levels were found in male, but not female, HZ mice (Figure 2G). Similar to their adolescent counterparts, 42-day-old male and female *Celsr3* HZ revealed increased grooming, even though this effect appeared more pronounced in males (Figure 2H). In addition, male *Celsr3* mutant males also had a higher occurrence of head and body jerks compared to male WT and female HZ mice (Figure 2I). No variations were observed in chewing, blinking, or digging behaviors across groups (Figures 2J-2L). Female mice displayed lower startle response than males (Figure 2M). Male HZ mice had lower acoustic PPI than WT males, a difference not seen in females (Figure 2N). Overall, these tests indicated a high level of face validity for *Celsr3* mutant mice with respect to key deficits observed in TS patients.

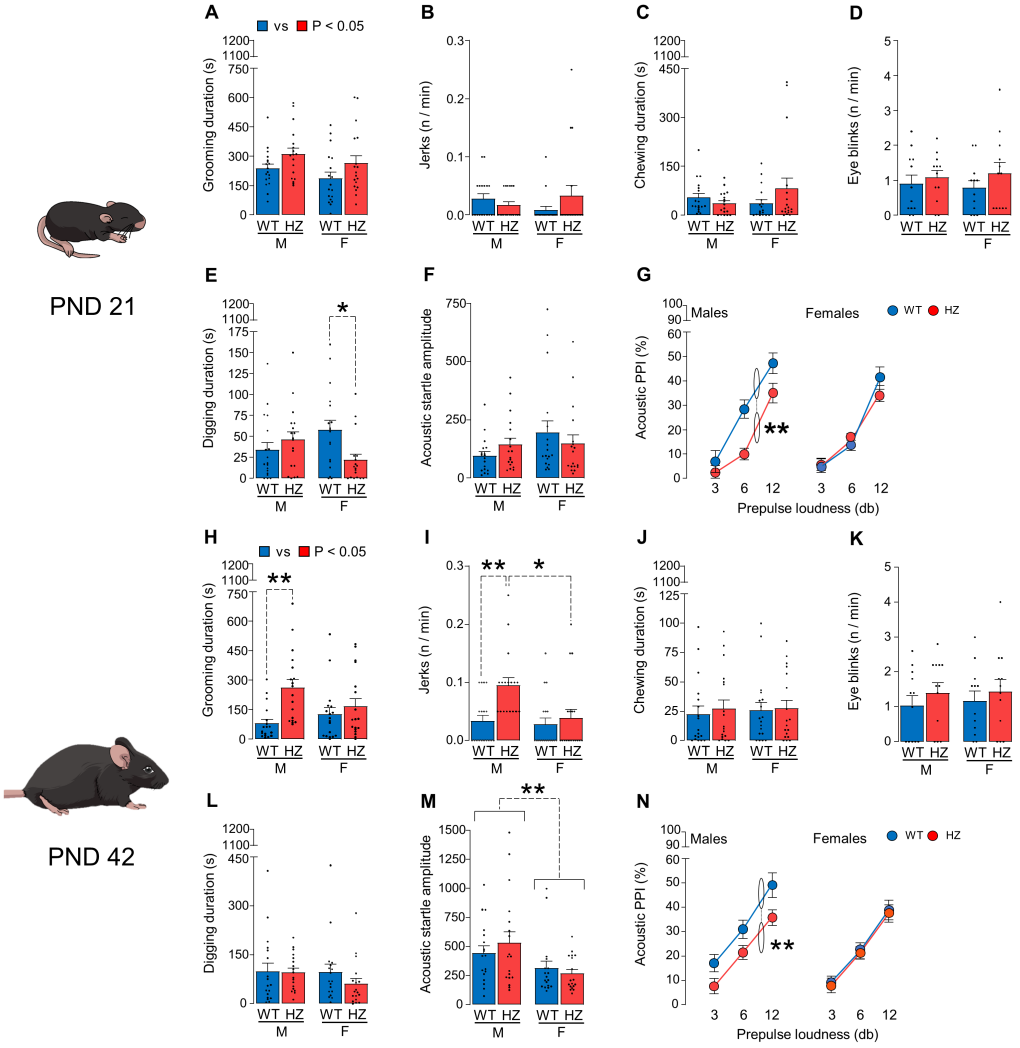


**Figure 2. Adolescent and juvenile *Celsr3* heterozygous (HZ) mice show spontaneous behavioral alterations related to Tourette syndrome (TS).** (A-G) Male and female *Celsr3* HZ mice were tested on postnatal day 21 (PND 21) for spontaneous TS-related behavioral alterations in comparison with wild-type (WT) littermates. Celsr3 mutant mice displayed a significant increase in spontaneous grooming (A), but not differences in the frequency of body and head jerks (B), chewing stereotypies (C), and eyeblink (D). Female HZ mice displayed a significant reduction in the overall duration of digging behavior (E). While no difference in the amplitude of the acoustic startle reflex was found (F), *Celsr3* HZ males, but not females, displayed significant prepulse inhibition (PPI) deficits (G). (H-N) Spontaneous behaviors were also assessed in a separate group of juvenile mice (PND 42). Grooming duration (H) was increased in HZ mice, and the effects were particularly marked for males. *Celsr3* HZ males also showed a significant increase in the frequency of jerks compared to male WT and female HZ mice (I). Chewing (J), eye-blinking (K), and digging behaviors (L) were similar for all groups. Irrespective of

genotype, males exhibited a significant increase in acoustic startle amplitude compared with females (M). However, only *Celsr3* HZ males displayed significant PPI deficits irrespective of the prepulse loudness (N). Data in panels G and N are presented as mean ± SEM for each sex and were analyzed by three-way ANOVA (for sex, genotype, and prepulse loudness). All other data are reported as mean ± SEM with individual data points and were analyzed by two-way ANOVA for sex and genotype (n=18/group, except for n=12/group for panels D and K). WT mice are indicated in blue, and HZ mice in red. *, $P<0.05$; **, $P<0.01$ for comparisons indicated by brackets. For further details, see text and Supplemental Information.

To verify whether these responses were accompanied by other behaviors related to comorbid diagnoses, we tested a separate cohort of juvenile (42- through 50-day-old) mice on a series of tests aimed at capturing complementary dimensions of behavioral reactivity (Figure 3). *Celsr3* HZ mice displayed increased locomotion (Figure 3A) and preference for the central area of an open field, irrespective of sex (Figure 3B). Unlike females, male HZ mice displayed deficits in the recognition of familiar objects (Figure 3C). Finally, no differences were detected in the marble-burying task, the elevated plus maze, or the suspended wire-beam bridge, which capture compulsive, anxiety-like, and impulsive responses (Figures 3D-3H).

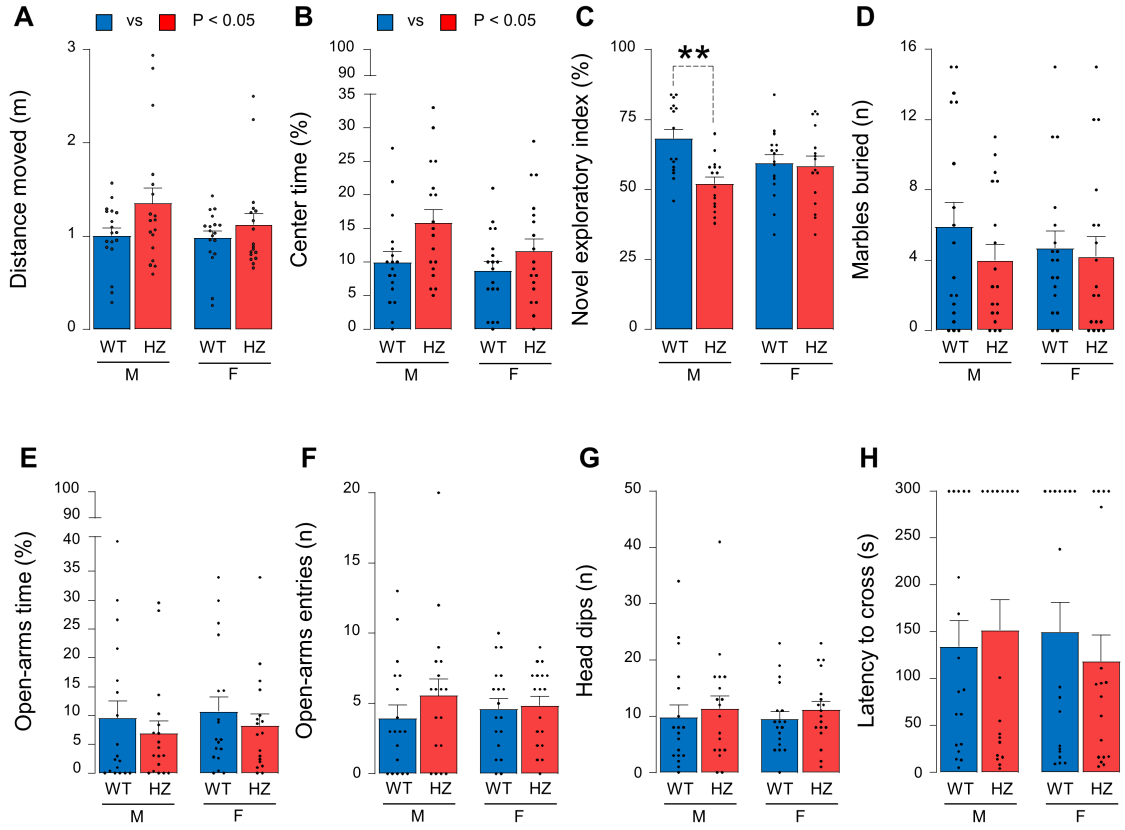


**Figure 3 *Celsr3* heterozygous (HZ) mice show comorbid hyperactivity and attentional deficits.** (A-B) Locomotor activity was monitored in a normal cage for 10 minutes. Evaluation of the average distance traveled (A) and the time spent in the center (B) showed a main effect for genotype, highlighting a hyperactive phenotype for *Celsr3* HZ mice. (C) Novel object recognition tests revealed a significant deficit in HZ males as compared to their wild-type (WT) counterparts (**, P<0.01). (D-H) No other differences between groups were identified independently of the paradigm used, whether it was to test compulsivity (marble burying, D), anxiety (elevated plus maze, E-G), or impulsivity (wire-beam elevated bridge test, H). Data are represented as means ± SEM with individual points. Data were analyzed with two-way ANOVA with genotype and sex as factors, followed by post-hoc analyses with Tukey´s correction (n=18/group, except for panel C, n=16/group). WT are indicated in blue and HZ in red. For further details, see text and Supplemental Information.

**TS-related deficits in *Celsr3* HZ male mice are exacerbated by stress and reduced by benchmark TS therapies.** Following this assessment, we evaluated the predictive validity of adult *Celsr3* HZ mice as a model of TS by testing whether relevant behavioral responses were modulated by environmental or pharmacological manipulations known to either exacerbate or reduce tic severity in patients. We first tested the effects of spatial confinement, an acutely stressful manipulation that has been shown to exacerbate tic-like and stereotyped responses in other models of TS [29,30]. When subjected to this manipulation, juvenile male and female HZ mice displayed elevated grooming responses, with males showing a more pronounced exacerbation (Figure S2A). Male HZ mice also manifested a higher frequency of body jerks irrespective of stress exposure (Figure S2B). An increase in startle amplitude was observed in male mice, irrespective of the genotype (Figure S2C); however, PPI deficits were only found in unstressed *Celsr3* HZ males, possibly due to a floor effect driven by stress exposure in all groups (Figure S2D).

We then tested the responsiveness of *Celsr3* HZ mice to different drugs known to reduce tic severity in TS. Our findings showed that the $D_2$ receptor antagonist haloperidol (0.25 mg/kg, IP) normalized grooming behavior, head jerks, and PPI, with no changes in startle amplitude (Figures 4A-4D). Similar improvements were produced by the $\alpha_2$ receptor agonist clonidine (0.25 mg/kg, IP; Figures 4E-4H) as well as the $D_1$ receptor antagonist ecopipam (0.5-1.0 mg/kg, IP; Figures 4I-4L), which has been recently shown to reduce tics in TS patients [29], and the 5α-reductase inhibitor finasteride (10 mg/kg, IP; Figures 4M-4P), which has been shown to reduce tics in patients and TS-related deficits in other models of tic disorders [28,30,31]. Taken together, these findings suggest that most TS-like manifestations in *Celsr3* mutants were exacerbated by acute stress and mitigated by several therapies for TS patients.

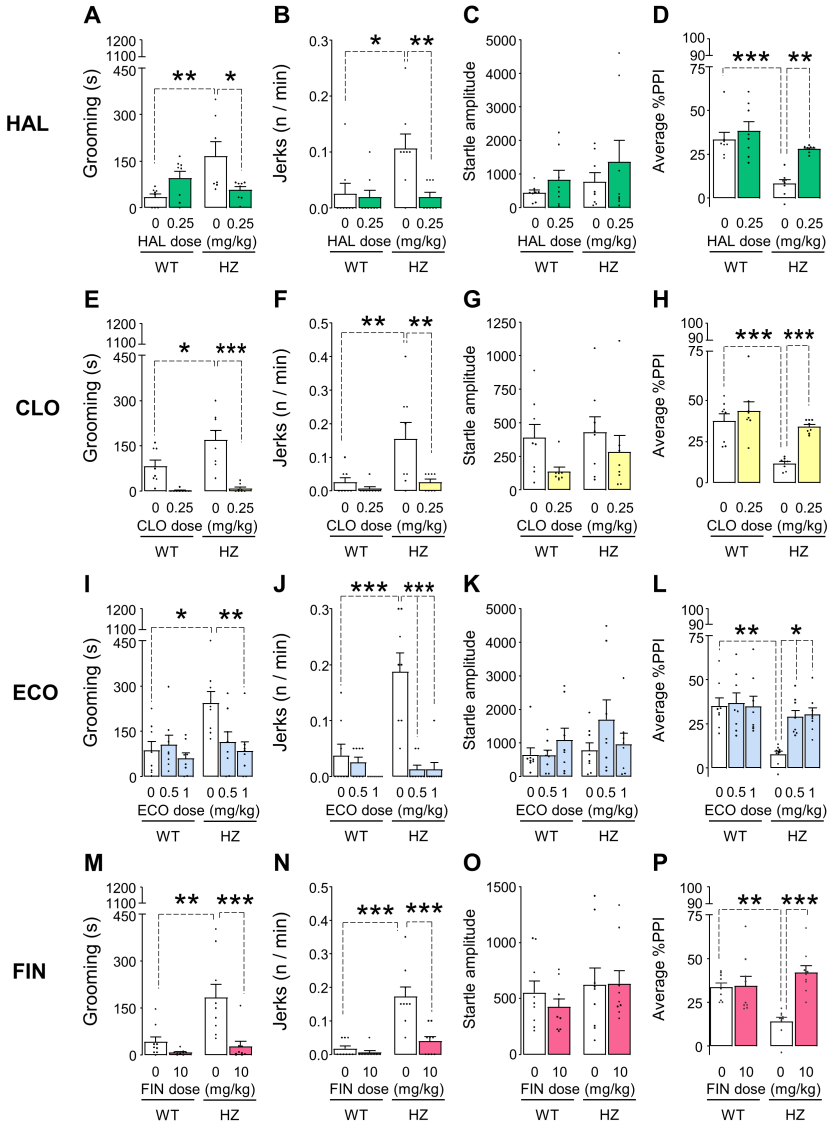


**Figure 4. Tourette syndrome therapies are effective against the spontaneous tic-like behaviors of *Celsr3* HZ mice.** (A-D) The antipsychotic haloperidol (HAL; 0.25 mg/kg, IP, injected 45 min before the behavioral assessment) rescued the spontaneous increases of grooming duration (A) and jerk frequency (B), as well as the PPI deficits, without affecting the startle reflex amplitude (C-D). (E-H) The $\alpha_2$ agonist clonidine (CLO; 0.25 mg/kg, IP, injected 30 min before testing) elicited similar effects, as shown by the analyses of grooming duration (E), jerk frequency (F), acoustic startle amplitude (G), and acoustic PPI (H). (I-L) Similar effects were induced by the $D_1$ receptor antagonist ecopipam (ECO; 0.5-1.0 mg/kg, IP, injected 20 min before testing), which reversed the spontaneous alterations of *Celsr3* HZ mice with respect to grooming duration (I), frequency of jerks (J), and PPI without affecting startle responses (K-L). (M-P) The 5α-reductase inhibitor finasteride (FIN; 10 mg/kg, IP, 30 min prior to testing) reduced the spontaneous grooming (M) and the frequency of jerks (N), while reversing the PPI deficits

in *Celsr3* HZ mice without affecting acoustic startle amplitude (O-P). All experiments were performed in male animals and were analyzed by two-way ANOVA, with genotype and treatment as factors, followed by post-hoc analyses with Tukey´s test (*, P<0.05; **, P<0.01; ***, P<0.001). All data are shown as means ± SEM (n=8-9/group). For further details, see text and Supplemental Information.

**Bulk transcriptomic studies identified significant changes in RNA processing and cytoskeleton regulation in striatal tissues from *Celsr3* HZ mice.** We then examined the transcriptomic differences in bulk striatal tissue between WT and HZ littermates, obtaining an average of 32.6 million (M) reads (range: 27.2 M – 39.4 M). The analyses (n=7/genotype), including RIN as a covariate, revealed 394 differentially expressed genes (DEGs), of which 226 were upregulated and 168 downregulated (Figures 5A-5B). Unbiased clustering of DEGs distinctly differentiated between WT and HZ (Figure 5C). As expected, *Celsr3* was one of the top genes whose expression was reduced in HZ mice ($\log_2$ FC = -0.817; FDR = 1.2E-03). Other significantly altered genes are implicated in Wnt signaling and cell cycle progression, and included *Tmed2, Chaserr, Slc7a5, Rpph1,* and *Ap4s1* (Table S1). Gene-ontology (GO) analysis found “cytoskeleton's structure” (GO:0005200), “molecular structure” (GO:0005198), and “cell-to-cell connections” (GO:0045171) as the most downregulated categories. In contrast, "mRNA processing" (GO:0006397), "RNA splicing" (GO:0008380), and "RNA splicing through transesterification reactions" (GO:0000375) were the most upregulated pathways (Figure 5D and Table S2). In line with these data, *Celsr3*-deficient mice displayed significant increases in the transcript levels of several genes involved in transcriptional regulation, such as *Gtf2h2, Zpf326, Tia1, Kansl1l,* and *Ube2b* (Table S2).

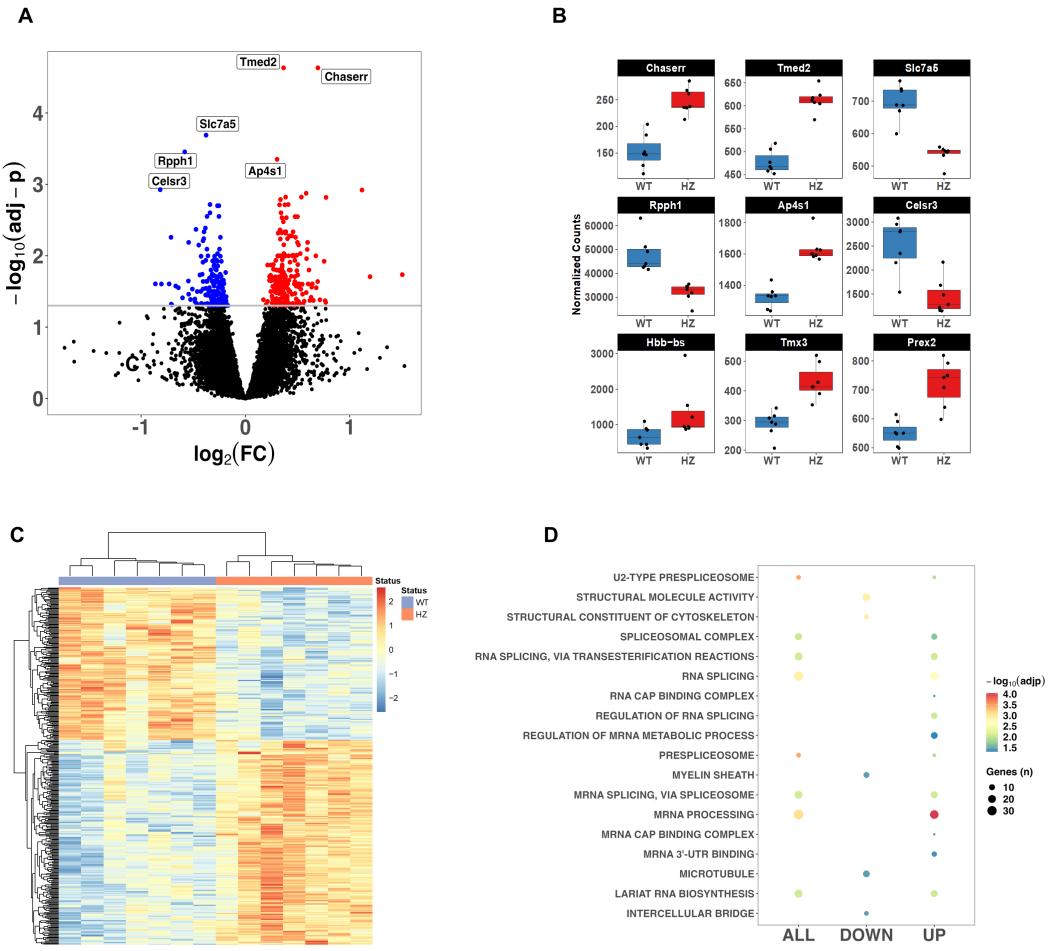


**Figure 5. Transcriptomic analyses of bulk striatal tissue of *Celsr3* heterozygous (HZ) and wild-type (WT) mice reveal differences in key metabolic processes.** (A) Volcano plot showing the differentially expressed genes (DEGs) between the *Celsr3* heterozygous (HZ, n=8) and wild-type (WT, n=8) striata. The top 6 DEGs are labeled. (B) Box plots showing the top 9 DEGs (HZ in red and WT in blue). (C) Heatmap generated with the Euclidean distance and Manhattan clustering method showing all the DEGs (FDR<0.05). (D) The results of gene ontology analyses using all the DEGs (all), only the downregulated (down), or only the upregulated (up) DEGs revealed that HZ mice showed differences in key processes, including the regulation of mRNA processing and metabolism, as well as microtubule regulation. For further details, see text and Supplemental Information.

**Single-nucleus (sn) transcriptomic studies highlighted subtle changes in striatal projection neurons (SPNs), interneurons, and microglia of *Celsr3* HZ mice**. As the comparisons between striatal tissues of *Celsr3* HZ and WT mice only showed broad functional differences, we employed sn-transcriptomics to identify cell-specific aberrances related to partial *Celsr3* deficiency (n=3/genotype). Using established cell markers, we categorized seven primary cell populations, including SPNs, interneurons, oligodendrocytes, astrocytes, microglia, ependymal and endothelial cells (Figures 6A-6B and S3, Tables S3 and S4). Notably, distinct differences in gene expression were evident in the SPN, interneuron, and microglia clusters (Figure 6C). In contrast, oligodendrocytes and other cell types exhibited minor transcriptomic variations between genotypes, suggesting their lower susceptibility to the effects of partial *Celsr3* deficiency (Figure 6C).

Within the SPN cluster, we identified 75 DEGs. GO analyses unveiled significant differences in various modules, including “negative regulation of protein phosphorylation” and “negative regulation of peptidyl-threonine phosphorylation” (Table S4). In another cluster, aligned with interneuron characteristics, we detected 130 DEGs with variations in pathways like "axon extension," “cell-cell adhesion,” and “neuron projection” (Table S4 and Figure S4). Finally, our analyses within microglial cells unveiled 92 DEGs and notable reductions in several GO pathways, including “synapse pruning,” “cell junction disassembly,” and “positive regulation of chemotaxis” (Table S4 and Figure S4).

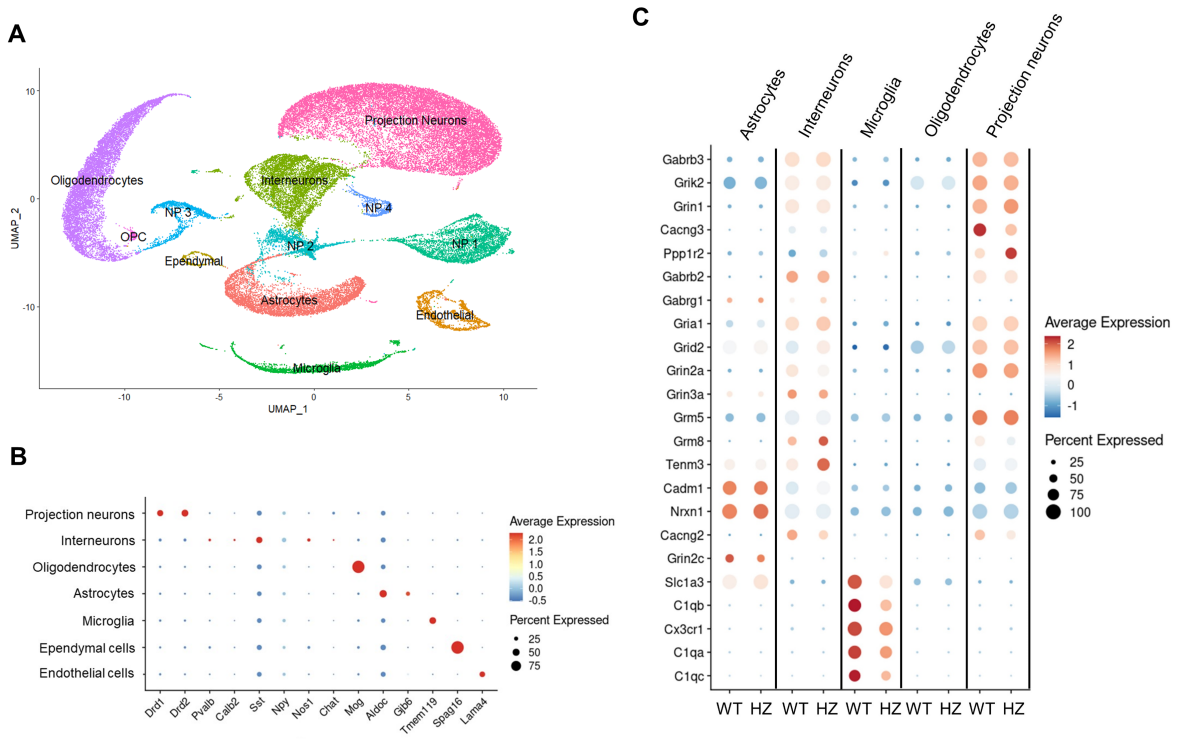


**Figure 6. Single-nucleus transcriptomic analyses of striatal tissues of *Celsr3* heterozygous (HZ) and wild-type (WT) mice reveal most differences in neuron and microglia clusters.** (A) Uniform Manifold Approximation and Projection (UMAP) of 48,834 nuclei annotated by major cell types, including astrocytes, oligodendrocytes, microglia, projection neurons, interneurons, progenitor cells (OPC), and other neuronal populations (NP 1-4). (B) Annotation of major clusters by select genes characteristic for major cell types. *Drd1* and *Drd2* expression is expected in projection neurons; *Pvalb, Calb2, Sst, Npy, Nos1*, and *Chat* as representative of several types of interneuron populations; *Mog* for mature oligodendrocytes; *Aldoc* and *Gjb6* for astrocytes; *Tmem119* for microglia; *Spag16* for ependymal cells; and *Lama4* for endothelial cells. (C) Dotplot of differential expression between wild-type (WT) and Celsr3 heterozygotes (HZ). Decreased expression is observed in several microglial-expressed genes related, some modest alterations in astrocytes, almost no changes in oligodendrocytes, but many alterations in glutamatergic and GABAergic pathways in the projection neurons and interneuron populations.

To understand which specific neuronal populations were most impacted by *Celsr3* deficiency, we revisited our snRNA-seq data using Gamma-Poisson modeling (Figure S5). This analysis allowed us to categorize six distinct SPN clusters and five distinct interneuron clusters (Figures 7A and S6, Tables S5 and S6), which were identified using established markers for each cell type (Figure 7B). The six SPN clusters included $D_1$-positive striosomal and matrisomal SPNs, $D_2$-positive striosomal and matrisomal SPNs, two unique clusters resembling eccentric “exopatch” neurons (e-SPNs). At an adjusted p-value $< 0.05$, most clusters only presented subtle alterations between genotypes (Figures 7C-7D). However, the smaller e-SPN cluster (e-SPN2) was mainly exclusive to *Celsr3* HZ mice, displaying heightened expressions of unique genes (Figure 7B), such as *Slc22a3* and *Slco5a1*. Compared with the larger e-SPN cluster, e-SPN2 cells showed an upregulation of microglia- and astrocyte-associated genes, suggesting that this subset of e-SPNs was characterized by abnormal development. Of the five interneuron clusters (Figures 7A-7B), calretinin-positive GABAergic interneurons (CRINs) exhibited the highest number of significant gene ontology alterations, including changes in “axon extension”, “axon guidance”, and “semaphorin receptor activity” (Figures 7C-7D). Minor modifications were also observed in other interneuron families, such as somatostatin-NPY-NOS2-positive interneurons (SNNINs) and parvalbumin-positive interneurons (PVINs) (Figures 7C-7D).

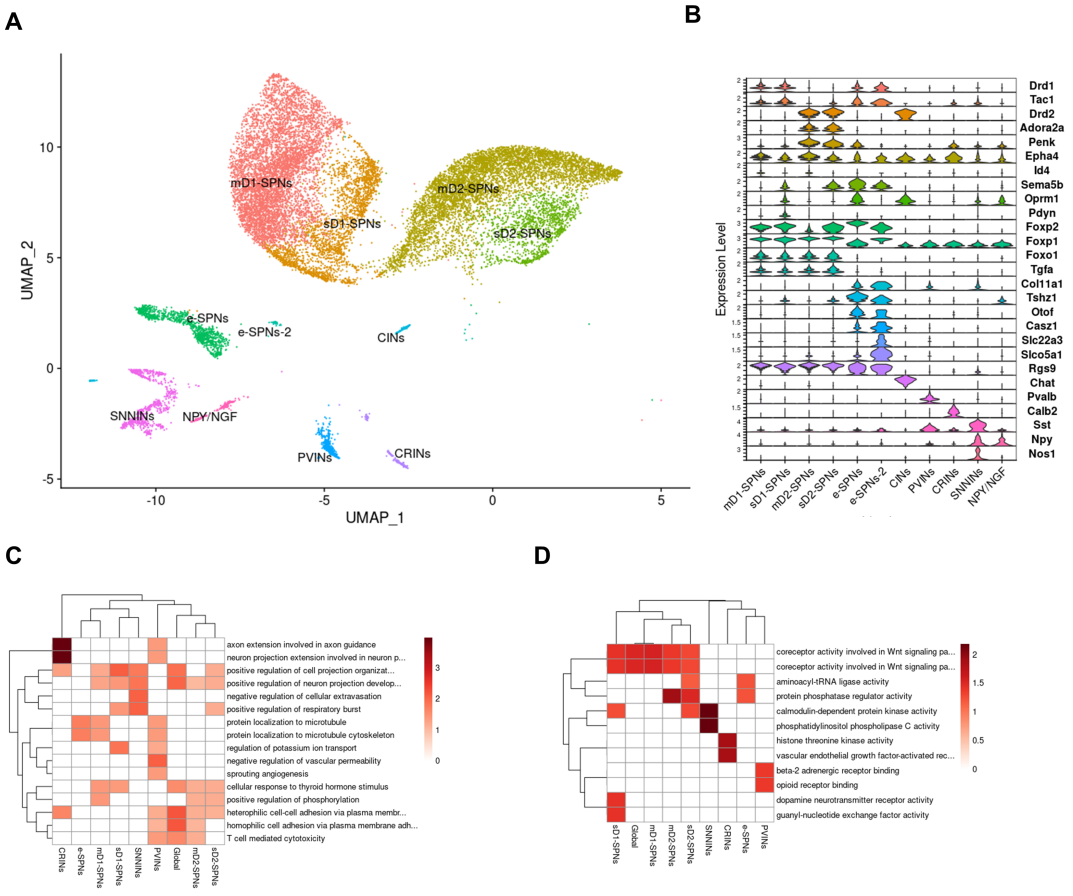


**Figure 7. Single-nucleus transcriptomic analyses of neuron-associated clusters of *Celsr3* heterozygous (HZ) and wild-type (WT) mice reveal a cluster of exopatch projection neurons almost exclusive to HZ mice, as well as marked differences in calretinin-positive interneurons.** (A) Uniform Manifold Approximation and Projection (UMAP) of projection neurons and interneuron populations following SCTransformation with the generalized linear model, Gamma Poisson method. The resolution of the clusters was chosen when they resolved into distinct clusters and evaluating clusters in clustree. (B) Violin plots of marker genes used to distinguish the select striatal clusters differentiating known cell types. (C-D) Gene ontology analysis highlighting the most differential ontologies among these cell clusters (C – GO biological process, and D – GO molecular function). Abbreviations: mD1-SPNs, matrisome-associated, $D_1$-positive striatal projection neurons; sD1-SPNs, striosome-associated, $D_1$-positive striatal projection neurons; mD2-SPNs, matrisome-associated, $D_2$-positive striatal projection neurons; sD2-SPNs, striosome-associated, $D_2$-positive striatal projection neurons; e-SPNs, eccentric striatal projection neurons (exopatch neurons); e-SPNs-2, eccentric striatal projection neurons (exopatch neurons), second cluster; CINs, cholinergic interneurons; SNNINs, somatostatin-NPY-NOS1-positive interneurons; NPY/NGF, NPY neurogliaform interneurons; PVINs, parvalbumin-positive interneurons; CRINs, calretinin-positive interneurons.

**Modulation of $D_3$ dopamine receptors modifies grooming and tic-like behaviors in *Celsr3* HZ mice.** Building on this evidence, we conducted a focused examination of the top 20 transcripts within each neuron cluster and compiled a comprehensive list of top DEGs (Figure 8A). This list featured 35 genes, including serine-threonine kinases (Sik2 and Sik3), key neurotrophin signaling molecules (including *Ntrk2,* encoding NT3 growth factor receptor, and its signaling effector *Shc3)*, myelin factors, such as *Mbp* (encoding myelin basic protein) and *Mobp* (myelin-associated oligodendrocyte basic protein), and thyroid hormone-binding targets including *Ttr* (transthyretin) and *Thrb* (thyroid hormone receptor beta). Furthermore, most cell types of *Celsr3* HZ mice featured the downregulation of the genes *Etv5* (encoding a transcription factor) and *Rpl29* (encoding a ribosomal protein). Notably, *Drd3* (encoding $D_3$ dopamine receptor) showed a striking upregulation in e-SPN2s and $sD_1$-SPNs and a concomitant reduction in CRINs (Figure 8A).

We hypothesized that alterations in $D_3$ receptors might contribute to the ontogeny of TS-related behavioral phenotypes in *Celsr3* HZ mice and be the most pharmacologically tractable target across those identified by our analyses, building on the concomitant reduction of $D_3$ receptor expression in CRINs (which contribute to local inhibitory mechanisms) and the increase in $D_1$-positive SPNs in patches and exopatches (which are posited to facilitate movements). To probe this hypothesis, we tested the effects of the selective $D_3$ receptor agonist PD 128907 (0.05 mg/kg, IP) and antagonist SB-277011A (10 mg/kg, IP) in TS-related alterations in these mutants. Activating the $D_3$ receptors with PD 128907 increased grooming stereotypies in HZ, but not WT, mice (Figure 8B), dramatically increased tic-like responses in both genotypes (Figure 8C), while it did not significantly impact startle amplitude and PPI (Figures 8D-8E). On the other hand, using the $D_3$ antagonist, SB-277011A, significantly reduced grooming in both WT and HZ mice (Figure 8F), reduced jerks in HZ, but not WT, mice (Figure 8G), without impacting the startle amplitude or PPI (Figures 8H-8I). Taken together, these data suggest that changes in cell-specific expression of $D_3$ receptors in the dorsal striatum are implicated in the stereotypies and tic-like manifestations observed in HZ mice. In contrast,

this receptor was not involved in the sensorimotor gating deficits exhibited by these mutants.

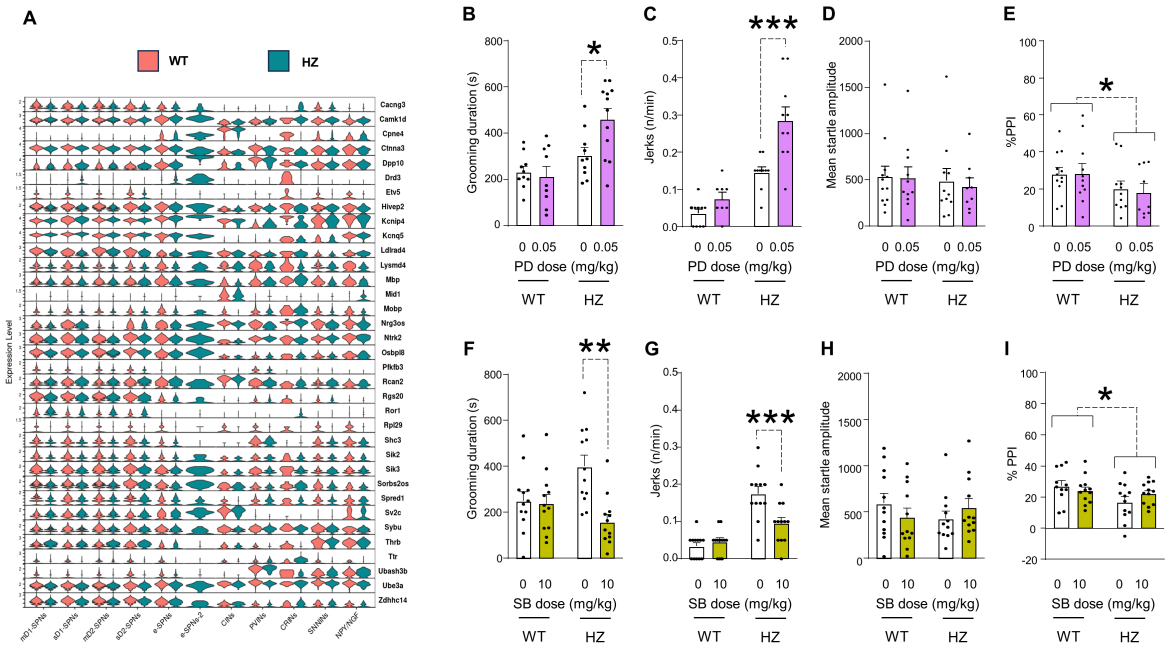


**Figure 8. Tic-like stereotypies and jerks in *Celsr3* heterozygous (HZ) mice are contributed by an expression shift in *Drd3* gene, encoding $D_3$ dopamine receptors**. (A) Violin plots of the top DEGs across all neuron clusters expressed in at least two cell types. All striatal cell types are shown. (B-I) Modulation of tic-related behaviors in *Celsr3* HZ mice treated either with the $D_3$ receptor agonist PD 128907 (PD) or the $D_3$ receptor antagonist SB 277011A (SB). All the alterations in tic-like behaviors spontaneously shown by Celsr3 mice were exacerbated by PD treatment (B-E) and rescued by SB treatment (F-I). Data in panel B-I are shown as means ± SEM (n=9/group) and were analyzed by two-way ANOVA, with genotype and treatment as factors, followed by post-hoc analyses with Tukey´s correction (*, P<0.05; **, P<0.01; ***, P<0.001). WT, wild-type.

## DISCUSSION

The purpose of this study was to characterize the phenotypic outcomes of *Celsr3* deficiency in animal models to verify their relevance to TS and other tic disorders. Although *Celsr3* HZ neonates exhibited similar responses to their WT counterparts, analyses in weanling and juvenile mice showed age- and sex-dependent abnormalities in *Celsr3* HZ mice. Specifically, these mutants exhibited an increased frequency of grooming stereotypies in both sexes (even though this aberrance became more pronounced in 42-day-old males); furthermore, male, but not female, juvenile HZ mice displayed an increased number of axial jerks and PPI deficits. The sex dimorphism of some of these behavioral alterations appears to mirror the male predominance of TS and aligns with similar differences observed in other TS mouse models, including D1CT-7 [32] and CIN-d mice [28], respectively featuring a neuropotentiating transgene in the somatosensory cortex and early-life depletion of striatal cholinergic interneurons (CIN-d) [28]. The examination of behavioral responses related to comorbid diagnoses revealed that *Celsr3* HZ mice exhibited elevated locomotor activity levels (in both sexes) and reduced object recognition (only in males). While we did not specifically measure attentional deficits, these aberrances align with the behavioral phenotype observed in rodent models of attention-deficit hyperactivity disorder (ADHD), a common comorbid condition observed in TS-affected individuals. These data point to the possibility that the behavioral outcomes of *Celsr3* deficiency may be relevant not only to TS but also to other concurrent neurodevelopmental disorders. Further investigations are required to gain a more comprehensive understanding of the role of *Celsr3* in regulating attention and other cognitive domains. Conversely, *Celsr3* HZ mice did not exhibit increased perseverative marble burying or anxiety-related behaviors, indicating that the stereotyped behaviors in these mice were not secondary to aberrances in these domains.

In line with ample evidence on the adverse effects of acute stress in TS [33] and in animal models of tic disorders, the severity of some of the behavioral abnormalities exhibited by HZ mice was exacerbated by spatial confinement, a mild contextual stressor that has been shown to elevate systemic synthesis of corticosterone [27] and brain production of

allopregnanolone [34]. Furthermore, most TS-related behavioral alterations were reduced by haloperidol and clonidine, two benchmark therapies for TS [35], and the $D_1$ dopamine receptor antagonist ecopipam, which was recently shown to significantly reduce tic severity and global functioning in TS patients [29]. Finally, we showed that TS-related responses were also reversed by finasteride, the steroidogenic inhibitor that was previously shown to ameliorate tic severity and other symptoms in an open study [30]. Notably, the effects of these drugs were specific to *Celsr3* HZ mice, pointing to the possibility that alterations in catecholamines and neuroactive steroids contribute to the TS-relevant behavioral alterations in these mutants. It should also be noted that these behavioral effects were observed after acute treatment, whereas these drugs exert therapeutic effects only after chronic administration in patients.

Taken together, this evidence suggests that *Celsr3*-deficient animals model tic disorders with high face, construct, and predictive validity. In particular, the fact that *Celsr3* deficiency produces tic-like behaviors in mice underscores the strong relevance of this gene in tic ontogeny. Furthermore, these data highlight *Celsr3* mutants as valid animal models of TS, which could be used to validate novel therapies and help improve understanding of the pathophysiology of this and other disorders.

Ample evidence suggests that tics are caused by the activation of aberrant foci in the striatum [36], which results from either excessive stimulation of medium spiny neurons or insufficient local inhibition (due to fewer or dysfunctional interneurons). Accordingly, a reduction in GABAergic parvalbumin-positive and somatostatin-positive, as well as cholinergic interneurons, has been documented in postmortem samples from TS-affected individuals [37,38].

We conducted transcriptomic analyses in striatal samples of HZ mice to gain a deeper understanding of the molecular mechanisms whereby *Celsr3* deficiency leads to TS-relevant phenotypes. Our transcriptomic analyses revealed widespread alterations in the RNA-processing machinery, including the upregulation of transcripts involved in mRNA processing and RNA slicing, spliceosome complex, and RNA cap binding complex. In addition, we found downregulations of transcripts involved in cytoskeleton and structural

activity, as well as microtubule regulation. These changes may signify alterations in neuronal development and neurite growth, two processes directly regulated by *Celsr3*.

Building upon these findings, we then performed sn-RNAseq of striatal cells from *Celsr3* HZ and WT mice, which revealed a complex network of subtle changes primarily affecting SPNs, CRINs, and microglia. Notably, *Celsr3* HZ mice exhibited a unique cluster of cells with characteristics highly overlapping with those of "exopatch" neurons (e-SPN), such as the expression of *Col11a1, Tshz1, Otof*, and *Casz1*. Exopatch neurons are physically located in the matrix but display properties and connectivity similar to $D_1$-positive striosomal neurons [39,40]. This minor e-SPN cluster differed from the other one due to the upregulation of several genes typically associated with microglia *(Apbb1ip, Inpp5d,* and *Mertk*) or astrocytes (*Nhsl1, Rorb*), opening the possibility that Ceslr3 deficiency may lead to aberrant development of a small subgroup of e-SPNs (here identified as a separate cluster). Our analyses also indicated other modifications in neurons, including changes in Wnt pathways and neurite guidance domains similar to those identified in the results of the bulk tissue analysis. Notably, previous studies have shown that *Celsr3* acts as a molecular guidepost, directing the migration of neurons along specific pathways and facilitating their precise positioning within neural circuits. *Celsr3* is also implicated in neurite growth. Neurites are crucial in establishing synaptic connections and forming functional neural networks. The observed changes in cytoskeleton and microtubule regulation align with the well-documented involvement of *Celsr3* and other genes included in the planar cell polarity (PCP) family in axon guidance and tract development [41]. Notably, axon guidance involves translating microenvironmental signals by the growth cone and controls the cytoskeleton. Furthermore, our analyses indicated that *Celsr3* deficiency impaired the ability of microglia to regulate synaptic pruning. The role of microglia in synaptic pruning has been shown to be critical for synaptic maturation [42]. Furthermore, dysfunctions of microglia and interneurons have been highlighted as crucial alterations in postmortem samples from individuals with high-severity TS [38]. The aberrations in striatal CRINs align with previous evidence indicating the malposition of these cells in the cortex of *Celsr3* knock-out embryos [26].

The integration of these abnormal processes might have culminated in the aberrant transcription of the *Drd3* gene, manifesting as a notable downregulation in CRINs and a concomitant upregulation in $sD_1$-MSNs, as well as the high expression of this gene in a cluster of eSPNs unique to *Celsr3* HZ mice. To the best of our knowledge, this study highlighted for the first time that, at least in mice, e-SPNs and CRINs have the highest physiological expression in *Drd3*. For the most part, $D_3$ receptors are poorly expressed physiologically in the striatum [43,44] and have been typically regarded as upregulated by pathological states associated with hyperkinetic manifestations. For example, enhanced expression of $D_3$ receptors has been linked to the emergence of tardive dyskinesias in primates [45]. Additionally, the upregulation of dopamine $D_3$ receptors in the striatum has been empirically shown to be instrumental in the genesis of dyskinetic manifestations [46], including levodopa-induced dyskinesias, specifically impacting $D_1$-SPNs [47].

Notably, recent evidence has shown that e-SPNs receive direct projections from the substantia nigra [40]. Given that $D_3$ receptors have the highest affinity for dopamine, partial deficiency of *Celsr3* may lead to a shift of $D_3$ expression onto striosomal $D_1$-SPNs and e-SPNs, leading to stereotypies and tic-like responses. In line with this notion, it should be noted that high activity in striosomes has been linked to increased stereotyped behavior [48]. In light of these findings, our data suggests that the upregulation of $D_3$ receptors in striosomal $D_1$-SPNs and a minor subcluster of e-SPNs might alter the effects of dopamine neurotransmission in the dorsal striatum, ultimately triggering motor stereotypies and tic-like jerks, albeit not sensorimotor gating deficits. Corroborating this observation, our studies revealed that selective activation and blockade of $D_3$ receptors exacerbated and mitigated grooming and tic-like alterations in HZ mice. Conversely, pharmacological modulation of this receptor was not associated with the sensorimotor gating deficits observed in *Celsr3* HZ mice, likely reflecting that the dorsal striatum is not primarily involved in the dopaminergic regulation of PPI. Substantiating whether the overexpression of $D_3$ receptors in patch and exopatch projection neurons plays a broader role in the predisposition to tics and related motor behaviors will necessitate further in-depth investigations.

Several limitations of our findings warrant attention. Firstly, it is important to acknowledge that while our results suggest a significant role of CRINs in tic-like responses in *Celsr3* HZ mice, the specific involvement of these cells in TS remains less clear. Previous investigations in postmortem dorsal striatal samples from individuals with TS have identified a notable reduction in large-size calretinin-positive interneurons, although medium-size calretinin-positive interneurons were unaffected [49]. Considering that large-size calretinin-positive cells largely overlap with cholinergic interneurons in primates [50], it remains uncertain whether deficits in specific CRIN subgroups are relevant to the etiology of TS. Moreover, caution should be exercised when extrapolating translational implications of our findings, given the substantial differences in the abundance, distribution, and functional significance of striatal CRINs between mice and primates [50]. Secondly, while our results indicate various functional changes in *Celsr3* HZ mice that may contribute to the development of tics, including alterations in $D_3$ receptor expression, they do not provide a precise mechanistic explanation of how *Celsr3* alterations contribute to the pathogenesis of neurodevelopmental disorders. These caveats notwithstanding, our results show that *Celsr3* deficiency leads to stereotyped behaviors and other tic-relevant manifestations in mouse models, with high face and predictive validity. These tic-like alterations are accompanied by aberrances in RNA processing machinery and cytoskeletal regulation in the striatum. Future research endeavors should aim to uncover the specific striatal alterations and downstream mechanisms that underpin the modifications observed in *Celsr3*-deficient models. Understanding the precise role of *Celsr3* in TS may contribute to developing targeted therapeutic interventions for individuals with this complex neurodevelopmental disorder.

Irrespective of the specific case of *Celsr3*, our data highlight that the combination of deep-phenotyping and transcriptomics in mice may represent a cost-effective, powerful platform to establish a functional genetic map of the numerous mutations associated with TS. Particularly when coupled with molecular profiling technology, this approach may enable us to establish how diverse genetic contributions to tic disorders may converge on common pathways and help elucidate the pathophysiological foundations of TS.

## MATERIALS AND METHODS

**Animals.** *Celsr3* mutant mice in C57BL/6J background were generated as previously reported [25]. As homozygous *Celsr3* knock-out mice die rapidly after birth [26], all studies were performed using heterozygous (HZ) and wild-type (WT) littermates, generated by breeding HZ sires with WT mothers. Given that the identified *de novo CELSR3* mutations in humans typically affect only one allele [19–21], the HZ genotype aligns with the alterations identified in TS-affected subjects. Housing facilities were maintained at 22°C, with lights on at 6:00 AM and lights off at 6:00 PM. Experimental manipulations were carried out between 9:00 AM and 4:00 PM. Every effort was made to minimize the number and suffering of animals. Thus, animal numbers for each experiment were determined through power analyses conducted on preliminary results. All experimental procedures were approved by the local Institutional Animal Care and Use Committees.

**Drugs**. Haloperidol, clonidine, and the $D_1$ receptor antagonist ecopipam were purchased from Sigma Aldrich (St. Louis, MO), were dissolved in 0.9% NaCl and administered IP before the behavioral testing (haloperidol: 0.25 mg/kg, 45 min before; clonidine: 0.25 mg/kg, 30 min before; ecopipam: 0.5-1.0 mg/kg, 20 min before). Finasteride (AstaTech, Bristol, PA), the selective $D_3$ receptor agonist PD 128907 (PD; Tocris Bioscience, Bristol, UK) and antagonist SB 277011A (SB; Cayman Chemical, Ann Arbor, MI) were dissolved in 2.5% DMSO, 2.5% Tween80, and 0.9% NaCl, and administered IP before the behavioral testing (FIN, 10mg/kg, 30 min before; PD, 0.05 mg/kg, 10 min before; SB, 10mg/kg, 20 min before). The injection volume for IP administration was 10 ml/kg.

**Behavioral assays.** As shown in Figure 1, behavioral assessments in *Celsr3* HZ mice and WT littermates were performed on males and females in three early developmental stages: newborn pups (postnatal days 1-7), weanlings (postnatal day 21), and juvenile (postnatal days 42-49) mice with different groups of mice to avoid developmental carryover effects. Behavioral assessment in newborn pups included righting and negative

geotaxis reflexes, ultrasonic vocalizations (on postnatal day 6), and locomotor activity (on postnatal day 7) [51].

In weanlings and juvenile mice, we evaluated spontaneous TS-relevant behavior, focusing on grooming, tic-like jerks, eye blinking, and prepulse inhibition of acoustic and tactile startle. Testing was carried out as previously described [51] (for more details, see Supplemental Methods). In addition, juvenile mice were tested for behavioral responses related to TS-comorbid diagnoses. Paradigms included open-field locomotor activity, novel object recognition, marble burying, elevated plus maze, and wire-beam bridge (for details, see Supplemental Methods).

Finally, separate cohorts of juvenile *Celsr3* HZ and WT male mice were used to study the impact of stress and the response to pharmacological treatments. To study the impact of stress, we subjected mice to spatial confinement, given that this mild stressor was shown to exacerbate TS-relevant responses in other mouse models [27,28]. To ensure deep phenotyping of fine motoric abnormalities, each test was conducted with at least two separate cameras with different orientations, and videos were monitored by personnel blinded to genotype and treatments with a 0.25-0.5 × speed. All procedural details are presented in the Supplemental Methods.

**Bulk transcriptomic analyses.** RNA was extracted from 16 male individuals, 8 WT and 8 *Celsr3 Hz,* using the RNeasy Lipid Tissue Mini Kit (Qiagen, Hilden, Germany). RNA purity was assessed by the $A_{260}/A_{280}$ absorbance ratio using a NanoDrop™ spectrophotometer (ThermoFisher Scientific, Waltham, MA). RNA was sequenced using a NovaSeq Reagent Kit v1.5_150x150 bp (100 M read-pairs) Sequencing (Illumina Inc, San Diego CA, USA) and sequencing libraries were prepared using Illumina TruSeq Stranded Total RNA Library Prep Ribo-Zero Gold kit (Illumina). Transcriptomic analyses on bulk tissues were performed as previously described [52]. For details, see Supplemental Methods.

**Single Nuclei Preparation and Transcriptomic Analyses.** Freshly dissected striata were immediately flash-frozen using liquid nitrogen and subsequently embedded in an Optimal Cutting Temperature (OCT; Tissue Plus, #4585, Fisher HealthCare, Waltham, MA) compound and stored at -80°C until further processing for nuclei extraction. Upon processing, specimens were gently thawed in 2 ml of ice-cold phosphate-buffered saline (PBS, devoid of Ca2+ and Mg2+). This solution was supplemented with various compounds: 0.54 μM Nectostatin (Inc. #J65341, ThermoFisher Scientific Chemicals, Waltham, MA), 1 μM HPN-07 (SML2163, Sigma-Aldrich), 0.32 μM sodium hydroxybutyrate (A1161314, ThermoFisher Scientific Chemicals), 78 nM Q-VD-Oph (SML0063, Sigma-Aldrich), and 0.2 U/ml of Ribolock RNase inhibitor (EO0381, Life Technologies Corporation, Carlsbad, CA). The tissue, held over dry ice in a 60-mm Petri dish, was methodically minced into fragments smaller than 2 mm using a razor blade. Subsequently, this tissue was transitioned to a 2 ml Dounce homogenizer containing 1.5 ml of nuclei extraction buffer (130-128-024, Miltenyi Biotec, Bergisch Gladbach, Germany) along with 0.2 U/ml Ribolock RNase inhibitor. The homogenization procedure consisted of ten strokes administered using pestle A, followed by ten more strokes with pestle B, and a 5-min incubation on ice. The process continued with twenty strokes using pestle B, a secondary 5-min incubation on ice, and concluded with another set of twenty strokes with pestle B. Samples were then centrifuged at 600×g for 5 min, resuspended in 400 μL of PBS enriched with 2% BSA, passed through a 70-μm FLOWMI for clarification, and strained via a 40-μm FLOWMI. Specimens were then entrusted to the Hunstman Cancer Institute High Throughput Genomics Core for 10X Genomics library construction and the subsequent sequencing stage.

The 10X Genomics Cell Ranger Single Cell pipeline was used to generate alignments and counts using the default and recommended parameters. Cell ranger's default mm 10 reference dataset was used for alignment. Seurat (4.1.0) was used for quality control and downstream analysis. Cells were filtered out based on having less than 750 genes and greater than 15 % mitochondrial genes. Genes were filtered out including a) mitochondrial genes; b) hemoglobin genes; and c) bias-producing genes, including *Gm42418, AY036118, Gm47283, Rpl26, Gstp1, Rpl35a, Erh, Slc25a5, Pgk1, Eno1, Tubb2a, Emc4,*

*Scg5, Ehd2, Espl1, Jarid1d, Pnpla4, Rps4y1, Xist, Tsix, Eif2s3y, Ddx3y, Uty, Kdm5d, Cmss1, AY036118,* and *Gm47283*. Dimensionality reduction was performed by finding nearest neighbors and clustering the data based on scaled RNA expression at a resolution of 0.1 to find primary cell types. Following this initial analysis, the data were processed including dimension reduction and clustering by SCTransformation (0.3.5) using the Gamma-Poisson generalized linear model (glmGamPoi, 1.4.0) method. A resolution 0.4 was chosen as the interneuron populations began separating into unique clusters. Cell subpopulations were identified for clusters using differential gene expression, and all manual annotations were compared to those produced through automated classification using SingleR (1.6.1) and enrichR (3.1, CellMarker Augmented 2021). Pathway and Gene Ontology analyses were performed with enrichR (3.1).

**Statistical analyses.** Normality and homoscedasticity of data distribution were verified using Kolmogorov-Smirnov and Bartlett's tests. Statistical analyses were performed using one- or multiway ANOVA, as appropriate. Post-hoc comparisons were performed by Tukey's test. Significance thresholds were set at 0.05. While only the main results of statistical analyses are presented in the text, all details are reported in Supplemental Results and Supplemental Tables.

## REFERENCES


1. Gorman DA, Thompson N, Plessen KJ, Robertson MM, Leckman JF, Peterson BS. Psychosocial outcome and psychiatric comorbidity in older adolescents with Tourette syndrome: controlled study. *The British Journal of Psychiatry*. 2010;197(1):36. doi:10.1192/BJP.BP.109.071050

2. Cooper C, Robertson MM, Livingston G. Psychological morbidity and caregiver burden in parents of children with Tourette's disorder and psychiatric comorbidity. *J Am Acad Child Adolesc Psychiatry*. 2003;42(11):1370-1375. doi:10.1097/01.CHI.0000085751.71002.48

3. Eddy CM, Rizzo R, Gulisano M, et al. Quality of life in young people with Tourette syndrome: a controlled study. *J Neurol*. 2011;258(2):291-301. doi:10.1007/S00415-010-5754-6

4. Eapen V, Cavanna AE, Robertson MM. Comorbidities, Social Impact, and Quality of Life in Tourette Syndrome. *Front Psychiatry*. 2016;7(JUN):97. doi:10.3389/FPSYT.2016.00097

5. Conelea CA, Woods DW, Zinner SH, et al. Exploring the impact of chronic tic disorders on youth: results from the Tourette Syndrome Impact Survey. *Child Psychiatry Hum Dev*. 2011;42(2):219-242. doi:10.1007/S10578-010-0211-4

6. American Psychiatric Association. (2013). Diagnostic and statistical manual of mental disorders (5th ed.). https://doi.org/10.1176/appi.books.9780890425596

7. Scharf JM, Miller LL, Gauvin CA, Alabiso J, Mathews CA, Ben-Shlomo Y. Population prevalence of Tourette syndrome: a systematic review and meta-analysis. *Mov Disord*. 2015;30(2):221-228. doi:10.1002/MDS.26089

8. Freeman RD, Fast DK, Burd L, Kerbeshian J, Robertson MM, Sandor P. An international perspective on Tourette syndrome: selected findings from 3,500 individuals in 22 countries. *Dev Med Child Neurol*. 2000;42(7):436-447. doi:10.1017/S0012162200000839

9. Leckman JF, Zhang H, Vitale A, et al. Course of tic severity in Tourette syndrome: the first two decades. *Pediatrics*. 1998;102(1 Pt 1):14-19. doi:10.1542/PEDS.102.1.14

10. Bloch MH, Leckman JF. Clinical course of Tourette syndrome. *J Psychosom Res*. 2009;67(6):497-501. doi:10.1016/J.JPSYCHORES.2009.09.002

11. Lebowitz ER, Motlagh MG, Katsovich L, et al. Tourette syndrome in youth with and without obsessive-compulsive disorder and attention deficit hyperactivity disorder.

*Eur Child Adolesc Psychiatry*. 2012;21(8):451-457. doi:10.1007/S00787-012-0278-5

12. Hirschtritt ME, Lee PC, Pauls DL, et al. Lifetime prevalence, age of risk, and genetic relationships of comorbid psychiatric disorders in Tourette syndrome. *JAMA Psychiatry*. 2015;72(4):325-333. doi:10.1001/JAMAPSYCHIATRY.2014.2650

13. Martino D, Ganos C, Pringsheim TM. Tourette Syndrome and Chronic Tic Disorders: The Clinical Spectrum Beyond Tics. *Int Rev Neurobiol*. 2017;134:1461-1490. doi:10.1016/BS.IRN.2017.05.006

14. Rizzo R, Gulisano M, Martino D, Robertson MM. Gilles de la Tourette Syndrome, Depression, Depressive Illness, and Correlates in a Child and Adolescent Population. *J Child Adolesc Psychopharmacol*. 2017;27(3):243-249. doi:10.1089/CAP.2016.0120

15. Billnitzer A, Jankovic J. Current Management of Tics and Tourette Syndrome: Behavioral, Pharmacologic, and Surgical Treatments. *Neurotherapeutics*. 2020;17(4):1681-1693. doi:10.1007/S13311-020-00914-6

16. Kompoliti K, Goetz CG, Morrissey M, Leurgans S. Gilles de la Tourette syndrome: patient's knowledge and concern of adverse effects. *Mov Disord*. 2006;21(2):248-252. doi:10.1002/MDS.20680

17. Jerrell JM, McIntyre RS. Adverse events in children and adolescents treated with antipsychotic medications. *Hum Psychopharmacol*. 2008;23(4):283-290. doi:10.1002/HUP.932

18. Felling RJ, Singer HS. Neurobiology of tourette syndrome: current status and need for further investigation. *J Neurosci*. 2011;31(35):12387-12395. doi:10.1523/JNEUROSCI.0150-11.2011

19. Willsey AJ, Fernandez T V., Yu D, et al. De Novo Coding Variants Are Strongly Associated with Tourette Disorder. *Neuron*. 2017;94(3):486-499.e9. doi:10.1016/J.NEURON.2017.04.024

20. Wang S, Mandell JD, Kumar Y, et al. De Novo Sequence and Copy Number Variants Are Strongly Associated with Tourette Disorder and Implicate Cell Polarity in Pathogenesis. *Cell Rep*. 2018;24(13):3441-3454.e12. doi:10.1016/J.CELREP.2018.08.082

21. Zhao X, Wang S, Hao J, Zhu P, Zhang X, Wu M. A Whole-Exome Sequencing Study of Tourette Disorder in a Chinese Population. *DNA Cell Biol*. 2020;39(1):63-68. doi:10.1089/DNA.2019.4746

22. Wang, X. J., Zhang, D. L., Xu, Z. G., Ma, M. L., Wang, W. B., Li, L. L., Han, X. L., Huo, Y., Yu, X., & Sun, J. P. (2014). Understanding cadherin EGF LAG seven-pass

G-type receptors. Journal of neurochemistry, 131(6), 699–711. https://doi.org/10.1111/jnc.12955

23. Tissir F, Bar I, Jossin Y, Goffinet AM. Protocadherin Celsr3 is crucial in axonal tract development. *Nat Neurosci*. 2005;8(4):451-457. doi:10.1038/NN1428

24. Jia Z, Guo Y, Tang Y, Xu Q, Li B, Wu Q. Regulation of the protocadherin Celsr3 gene and its role in globus pallidus development and connectivity. *Mol Cell Biol*. 2014;34(20):3895-3910. doi:10.1128/MCB.00760-14

25. Wu S, Ying G, Wu Q, Capecchi MR. A protocol for constructing gene targeting vectors: generating knockout mice for the cadherin family and beyond. *Nat Protoc*. 2008;3(6):1056-1076. doi:10.1038/NPROT.2008.70

26. Ying G, Wu S, Hou R, Huang W, Capecchi MR, Wu Q. The protocadherin gene Celsr3 is required for interneuron migration in the mouse forebrain. Mol Cell Biol. 2009 Jun;29(11):3045-61. doi: 10.1128/MCB.00011-09.

27. Godar SC, Mosher LJ, Strathman HJ, et al. The D1CT-7 mouse model of Tourette syndrome displays sensorimotor gating deficits in response to spatial confinement. *Br J Pharmacol*. 2016;173(13):2111-2121. doi:10.1111/BPH.13243

28. Cadeddu, R., Van Zandt, M., Santovito, L. S., Odeh, K., Anderson, C. J., Flanagan, D., Nordkild, P., Pinna, G., Pittenger, C., & Bortolato, M. (2023). Prefrontal allopregnanolone mediates the adverse effects of acute stress in a mouse model of tic pathophysiology. Neuropsychopharmacology, 48(9), 1288–1299. https://doi.org/10.1038/s41386-023-01603-6

29. Gilbert DL, Dubow JS, Cunniff TM, Wanaski SP, Atkinson SD, Mahableshwarkar AR. Ecopipam for Tourette Syndrome: A Randomized Trial. Pediatrics. 2023 Feb 1;151(2):e2022059574. doi: 10.1542/peds.2022-059574. PMID: 36628546.

30. Muroni A, Paba S, Puligheddu M, Marrosu F, Bortolato M. A preliminary study of finasteride in Tourette syndrome. *Mov Disord*. 2011;26(11):2146-2147. doi:10.1002/MDS.23810

31. Mosher LJ, Godar SC, Nelson M, Fowler SC, Pinna G, Bortolato M. Allopregnanolone mediates the exacerbation of Tourette-like responses by acute stress in mouse models. *Scientific Reports 2017 7:1*. 2017;7(1):1-9. doi:10.1038/s41598-017-03649-1

32. Nordstrom EJ, Burton FH. A transgenic model of comorbid Tourette's syndrome and obsessive-compulsive disorder circuitry. *Mol Psychiatry*. 2002;7(6):617-625. doi:10.1038/SJ.MP.4001144

33. Godar, S. C., & Bortolato, M. (2017). What makes you tic? Translational approaches to study the role of stress and contextual triggers in Tourette syndrome. Neuroscience and biobehavioral reviews, 76, 123–133. https://doi.org/10.1016/j.neubiorev.2016.10.003

34. Mosher, L. J., Cadeddu, R., Yen, S., Staudinger, J. L., Traccis, F., Fowler, S. C., Maguire, J. L., & Bortolato, M. (2019). Allopregnanolone is required for prepulse

inhibition deficits induced by D1 dopamine receptor activation. Psychoneuroendocrinology, 108, 53–61. https://doi.org/10.1016/j.psyneuen.2019.06.009

35. Egolf A, Coffey BJ. Current pharmacotherapeutic approaches for the treatment of Tourette syndrome. *Drugs Today (Barc)*. 2014;50(2):159-179. doi:10.1358/DOT.2014.50.2.2097801

36. Albin, R. L., & Mink, J. W. (2006). Recent advances in Tourette syndrome research. Trends in neurosciences, 29(3), 175–182. https://doi.org/10.1016/j.tins.2006.01.001

37. Kalanithi PSA, Zheng W, Kataoka Y, et al. Altered parvalbumin-positive neuron distribution in basal ganglia of individuals with Tourette syndrome. *Proc Natl Acad Sci U S A*. 2005;102(37):13307-13312. doi:10.1073/PNAS.0502624102

38. Lennington JB, Coppola G, Kataoka-Sasaki Y, et al. Transcriptome analysis of the human striatum in Tourette syndrome. *Biol Psychiatry*. 2016;79(5):372. doi:10.1016/J.BIOPSYCH.2014.07.018

39. Smith JB, Klug JR, Ross DL, et al. Genetic-based dissection unveils the inputs and outputs of striatal patch and matrix compartments. *Neuron*. 2016;91(5):1069. doi:10.1016/J.NEURON.2016.07.046

40. Märtin A, Calvigioni D, Tzortzi O, Fuzik J, Wärnberg E, Meletis K. A Spatiomolecular Map of the Striatum. *Cell Rep*. 2019;29(13):4320-4333.e5. doi:10.1016/J.CELREP.2019.11.096

41. Tissir F, Goffinet AM. Atypical cadherins Celsr1-3 and planar cell polarity in vertebrates. *Prog Mol Biol Transl Sci*. 2013;116:193-214. doi:10.1016/B978-0-12-394311-8.00009-1

42. Paolicelli RC, Bolasco G, Pagani F, et al. Synaptic pruning by microglia is necessary for normal brain development. *Science (1979)*. 2011;333(6048):1456-1458. doi:10.1126/SCIENCE.1202529/SUPPL_FILE/PAOLICELLI.SOM.PDF

43. Sokoloff P, Giros B, Martres MP, Bouthenet ML, Schwartz JC. Molecular cloning and characterization of a novel dopamine receptor (D3) as a target for neuroleptics. *Nature*. 1990;347(6289):146-151. doi:10.1038/347146A0

44. Levesque D, Diaz J, Pilon C, et al. Identification, characterization, and localization of the dopamine D3 receptor in rat brain using 7-[3H]hydroxy-N,N-di-n-propyl-2-aminotetralin. *Proc Natl Acad Sci U S A*. 1992;89(17):8155-8159. doi:10.1073/PNAS.89.17.8155

45. Mahmoudi S, Lévesque D, Blanchet PJ. Upregulation of dopamine D3, not D2, receptors correlates with tardive dyskinesia in a primate model. *Mov Disord*. 2014;29(9):1125-1133. doi:10.1002/MDS.25909

46. Cote SR, Chitravanshi VC, Bleickardt C, Sapru HN, Kuzhikandathil E V. Overexpression of the dopamine D3 receptor in the rat dorsal striatum induces

dyskinetic behaviors. *Behavioural brain research*. 2014;263:46-50. doi:10.1016/J.BBR.2014.01.011

47. Solís O, Garcia-Montes JR, González-Granillo A, Xu M, Moratalla R. Dopamine D3 Receptor Modulates l-DOPA-Induced Dyskinesia by Targeting D1 Receptor-Mediated Striatal Signaling. *Cereb Cortex*. 2017;27(1):435-446. doi:10.1093/CERCOR/BHV231

48. Canales JJ, Graybiel AM. A measure of striatal function predicts motor stereotypy. *Nature Neuroscience 2000 3:4*. 2000;3(4):377-383. doi:10.1038/73949

49. Kataoka Y, Kalanithi PS, Grantz H, Schwartz ML, Saper C, Leckman JF, Vaccarino FM. Decreased number of parvalbumin and cholinergic interneurons in the striatum of individuals with Tourette syndrome. J Comp Neurol. 2010 Feb 1;518(3):277-91. doi: 10.1002/cne.22206. PMID: 19941350; PMCID: PMC2846837.

50. Petryszyn, S., Di Paolo, T., Parent, A., & Parent, M. (2016). The number of striatal cholinergic interneurons expressing calretinin is increased in parkinsonian monkeys. Neurobiology of disease, 95, 46–53. https://doi.org/10.1016/j.nbd.2016.07.002

51. Godar SC, Mosher LJ, Scheggi S, et al. Gene-environment interactions in antisocial behavior are mediated by early-life 5-HT 2A receptor activation. *Neuropharmacology*. 2019;159. doi:10.1016/J.NEUROPHARM.2019.01.028

52. Piras IS, Braccagni G, Huentelman MJ, Bortolato M. A preliminary transcriptomic analysis of the orbitofrontal cortex of antisocial individuals. *CNS Neurosci Ther*. Published online 2023. doi:10.1111/CNS.14283